Journal of Electrical Engineering & Technology (2022) 17:351–360
https://doi.org/10.1007/s42835-021-00875-6

ORIGINAL ARTICLE

Torque Ripple Reduction of BLDC Traction Motor of Electric Wheelchair for Ride Comfort Improvement

Dae-Kee Kim[1] · Dong-Min Kim[2] · Jin-Cheol Park[1] · Soo-Gyung Lee[3] · Jihyung Yoo[1] · Myung-Seop Lim[1]

Received: 9 November 2020 / Revised: 6 April 2021 / Accepted: 12 August 2021 / Published online: 20 September 2021
© The Korean Institute of Electrical Engineers 2021, corrected publication 2021

Abstract

In this study, a method to reduce the torque ripple of brushless direct current (BLDC) traction motor which drives the electric wheelchair is discussed. As the main users of electric wheelchair are mobility handicapped people, it is important to decrease the speed ripple of the wheelchair for their comfort and safety and for this, reducing the torque ripple of traction motor can be a solution for this problem, because the fluctuation of vehicle speed is affected by ripple of the driving torque, especially at lower speed. The waveforms of current and back electromotive force (EMF) of motor need to be considered because they determine the torque characteristics such as average value and ripple. After the current waveform of BLDC motor is calculated by simulation, back EMF waveform that reduces the torque ripple is determined as a trapezoidal form. The traction motor for electric wheelchair reducing torque ripple is designed by optimization process. The design parameter selected from the sensitivity analysis are optimized through kriging surrogate model. Finally, the back EMF waveform and the torque ripple of BLDC motor are verified by conducting experiments.

Keywords Back EMF · BLDC motor · Torque ripple · Electric wheelchair

1 Introduction

The vehicles such as wheelchairs for mobility disabled people, have served as the assistant by providing mobility to such people. Recently, demands for comfort have made such vehicles to be powered by electricity. For example, in case of conventional wheelchair, the power to drive the vehicle is provided either by the passengers themselves or by other people which can be quite troublesome for passengers. Therefore, providing the power to the wheelchair by electric motor can help them overcome this discomfort. With the traction force generated by the electric motor, the passengers can move without driving the wheelchair by themselves or by other people. Thus, electric wheelchair can offer more convenience to its passengers than conventional wheelchair.

Because the main users of the electric wheelchair are either mobility disabled or are elderly people, the vehicle speed fluctuation should be reduced for their ride comfort and safety because this can cause difficulties for them to cope with uncomfortable and unexpected situations. Thus, several research studies have been conducted to make passengers of electric wheelchair comfortable. The regenerative braking control during downhill drive of electric wheelchair for securing safety was discussed in [1], and the drive controlling method considering road disturbances was discussed in [2]. Reference [3] focused on the uphill control method for driving electric wheelchair, and other control methods for electric wheelchair such as electromyographic-based control [4] and power-assist control [5] have been discussed. While

✉ Myung-Seop Lim
myungseop@hanyang.ac.kr

Dae-Kee Kim
haunters@hanyang.ac.kr

Dong-Min Kim
kimdmin@honam.ac.kr

Jin-Cheol Park
skensk1990@hanyang.ac.kr

Soo-Gyung Lee
soogyunglee@posco.com

Jihyung Yoo
jihyungyoo@hanyang.ac.kr

[1] Department of Automotive Engineering, Hanyang University, Seoul, Republic of Korea

[2] Department of Automotive Engineering, Honam University, Gwangju, Republic of Korea

[3] Steel Solution R&D Center, POSCO, Incheon, Republic of Korea

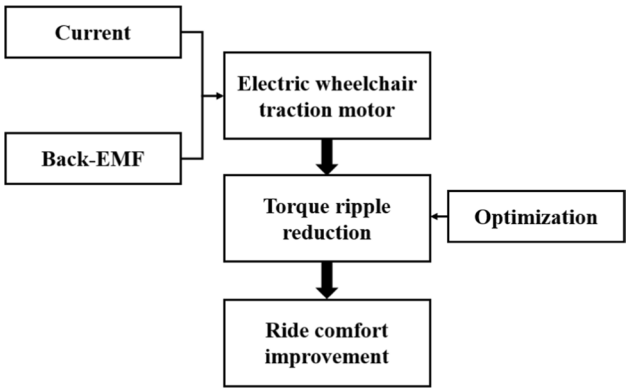

Fig. 1 Overall process of ride comfort improvement of electric wheelchair by reducing the motor torque ripple

most of the studies on electric wheelchair focused on control methods of electric wheelchair [6], focused on improving the characteristics of electric traction motor that provides the traction force to electric wheelchair. This study focused on reducing the torque ripple by minimizing the cogging torque by optimizing the air gap of motor.

This study focused on improving the performance of electric traction motor by improving the ride comfort of electric powered wheelchair. The torque ripple of brushless direct current (BLDC) motor that drives the electric wheelchair is minimized to reduce the speed ripple of wheelchair resulting in the ride comfort improvement. Figure 1 shows the overall process. First, the relationship between the torque ripple of motor and speed ripple of electric wheelchair, which is directly related to the ride comfort, is discussed. Subsequently, the waveforms of current and back-electromotive force (EMF) are considered, because torque characteristics of motor is determined by these waveforms. The current waveform of BLDC motor is calculated by simulation, and back EMF waveform that decreases the torque ripple is selected. The traction motor for electric wheelchair is designed by optimization process to reduce torque ripple. Several design parameters for optimization are selected by sensitivity analysis. These parameters are optimized using kriging surrogate model. The experiments on the BLDC traction motor for analyzing back EMF waveform, and torque ripple is conducted.

2 Relationship Between Torque Ripple of Electric Motor and Speed Ripple of Electric Wheelchair

The electric wheelchair speed ripple can cause inconvenience to the passengers, so it is important to remove it for ride comfort improvement. Since the electric motor provides the electric wheelchair with mobility by traction torque, the speed ripple can be affected by torque characteristics of motor. This section discusses the relationship between torque ripple of electric motor and fluctuation of wheelchair speed.

2.1 Electric Wheelchair Modeling

The driving torque generated by motor can be converted into traction force that makes the electric wheelchair move. Then, speed ripple can be calculated considering the correlation between traction force and wheelchair speed. The driving torque is transmitted to wheel through shaft with gear box as shown in Fig. 2. Each wheel is driven by a BLDC motor. T_D is the average driving torque of the motor, T_r is torque ripple, T_L represents load torque, n_G is gear ratio, z_a is number of teeth of input gear and z_b is that of output gear. As shown in Fig. 2, the relationship between torque and force can be written as (1) where r is the wheel radius, F_{TR} is total resistance force and F_T is traction force acting on the vehicle.

$$(T_D + T_r - T_L)n_G = r\left(F_T - F_{TR}\right) \tag{1}$$

The speed of the vehicle v can be calculated using (2). t stands for time, m_v is the mass of the vehicle, and m_{eq} is the equivalent mass of rotating parts such as motor and wheel which can be obtained using (3). J_m and J_w are the moment of inertia of traction motor and wheel, respectively and F is the net force.

$$v(t) = \frac{1}{(m_v + m_{eq})}\int_0^t F(t)dt \tag{2}$$

$$m_{eq} = \left(J_w + n_G^2 J_m\right)\left(\frac{1}{r}\right)^2 \tag{3}$$

2.2 Simulation Results and Analysis

By applying (1)–(3), the speed ripple of electric wheelchair is calculated. Figure 3 shows the process of calculating

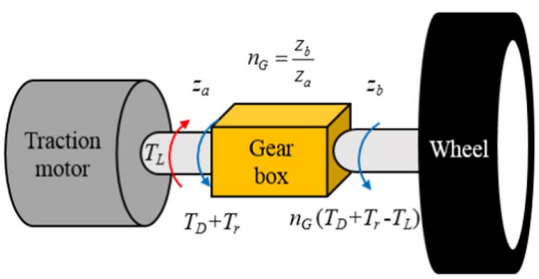

Fig. 2 Traction motor torque transmitting through shaft to wheel of the vehicle

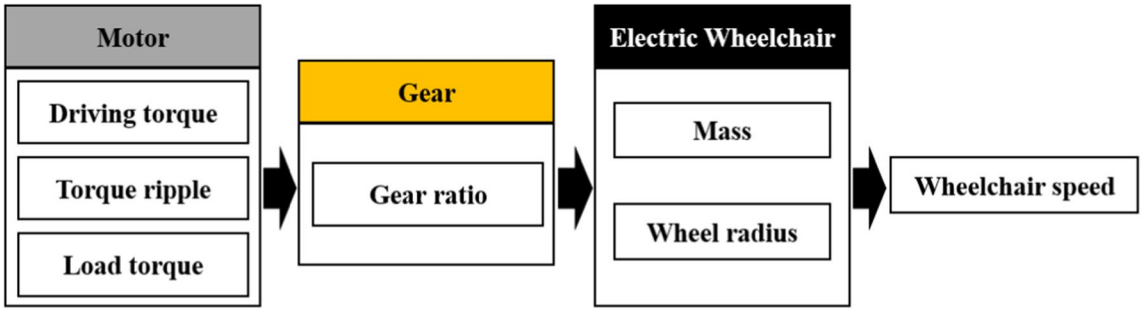

Fig. 3 Schematic diagram of wheelchair speed simulation

Table 1 Specifications of reference electric wheelchair

	Value	Unit
Vehicle weight	58	kg
Gear ratio	15	–
Width	0.66	m
Height	0.82	m
Wheel diameter	0.41	m

wheelchair speed. To determine the average speed region where torque ripple is more effective on speed ripple, the changes in wheelchair speed is calculated depending on different speed with same torque, and different amplitude of torque ripple is applied in same average wheelchair speed to verify the effect of torque ripple on speed ripple. The range of motor speed for verification is determined by considering the maximum speed of electric wheelchair. The electric wheelchair has limited speed range for safety. According to UK government, powered wheelchairs and scooters must not travel faster than 6 km/h on pavements or in pedestrian areas by Rule 39 [7]. Considering the relationship between motor rotating speed N_m and vehicle speed v in (4), the motor speed at maximum vehicle speed is 1175 rpm. The unit of rotating speed is rpm and unit of vehicle speed is km/h. Thus, the speed range of motor for verification is determined as below 1200 rpm.

$$v = \frac{60N_m}{1000n_G} \times 2\pi r \tag{4}$$

The specifications of electric wheelchair are listed in Table 1 [8]. The vehicle weight is 58 kg, the gear ratio is 15, the wheelchair width and height is 0.66 m and 0.82 m each, and the wheel radius is 0.41 m. Some assumptions were applied to this simulation. The cargo mass is 100 kg, the average speed of wheelchair is constant, and the number of wheels of wheelchair is 2 therefore the wheelchair is driven by 2 motors.

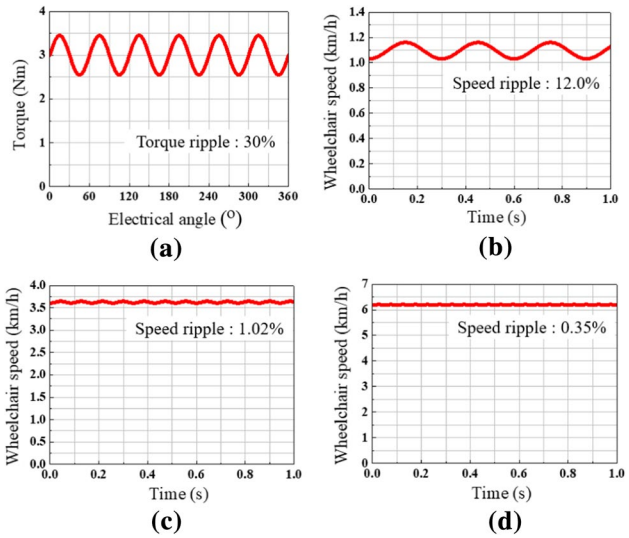

Fig. 4 **a** Torque waveform applied on electric wheelchair model and speed ripple of wheelchair depending on motor speed **b** 200 rpm, **c** 700 rpm, **d** 1200 rpm

Table 2 Changes in speed ripple of the wheelchair depending on motor speed

Motor speed (rpm)	Torque ripple (%)	Average wheelchair speed (km/h)	Speed ripple (%)
200	30	1.08	12.0
700	30	3.57	1.02
1200	30	6.12	0.35

Figure 4 and Table 2 show the simulation result of speed ripple change depending on motor rotating speed applying same torque ripple and the value is 30%. Figure 4a shows the applied motor torque waveform and the others show the speed ripple of wheelchair with different wheelchair speed. In Table 2, the average wheelchair speed at each motor speed is calculated with speed ripple. When motor rotates at 1200 rpm which is nearly maximum speed

of electric wheelchair, the speed ripple drops from 12.0 to 0.35% compared with at 200 rpm. This drastic change indicates that torque ripple by traction motor at relatively low speed affect the speed ripple more than at relatively high speed.

On the other hand, Fig. 5 and Table 3 show the simulation result of speed ripple change depending on torque ripple amplitude with same motor speed. Figure 5a is the applied motor torque waveform with different torque ripple and the others show the fluctuation of speed depending on the torque ripple with same motor speed of 200 rpm. According to Table 3, as the torque ripple is decreased from 50 to 30%, the speed ripple drops from 19.2 to 12.0%. This indicates that lower torque ripple of motor reduces the speed ripple. Therefore, considering these simulation results, reducing the torque ripple at relatively low speed effectively reduce the speed ripple resulting in the improvement of ride comfort of electric wheelchair.

3 Current and Back EMF Waveform for Reduction of Speed Ripple of Electric Wheelchair

As the improvement of ride comfort of vehicle can be obtained by reducing the torque ripple, several factors that affect the torque ripple are discussed in this section along with electrical input such as current and back EMF. The torque ripple reduction is mainly considered at 200 rpm of motor speed, because torque ripple is more effective to reduce speed ripple at lower speed.

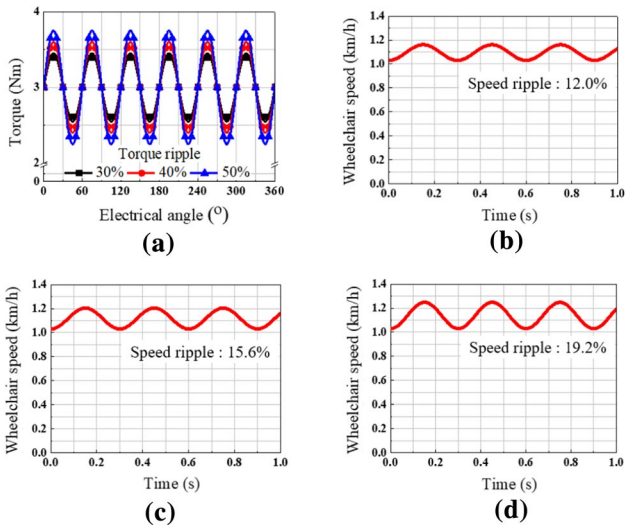

Fig. 5 **a** Torque waveform applied on electric wheelchair model at different ripple and speed ripple of wheelchair depending on torque ripple **b** 30% **c** 40% **d** 50%

Table 3 Changes in speed ripple of the wheelchair depending on motor speed

Motor speed (rpm)	Torque ripple (%)	Average wheelchair speed (km/h)	Speed ripple (%)
200	30	1.08	12.0
200	40	1.08	15.6
200	50	1.08	19.2

3.1 Current Waveform of BLDC Motor

The torque generated by motor can be obtained by (5), where m indicates the number of phases, e is back EMF, i means current, t is time, T represents torque and ω is rotating speed of motor. This implies that the characteristics of electrical input such as current and back EMF can influence the torque ripple.

$$m \cdot e \cdot i = T \cdot \omega \tag{5}$$

Initially, to determine the torque ripple of BLDC motor, the characteristics of current waveform should be considered. This can be calculated by simulation of electric circuit of BLDC motor considering switching sequence [9]. The information of circuit parameter is presented in Table 4. Then, the current waveform at 200 rpm of motor speed is obtained as shown in Fig. 6, of which the form is nearly square wave.

3.2 Speed Ripple Depending on the Waveform of Back EMF

The waveform of back EMF also significantly affects the torque characteristics in (5). Considering the current waveform in Fig. 6, appropriate back EMF waveform for reducing torque ripple should be selected. In general, two types of back EMF waveform can be considered, trapezoidal and sinusoidal. Figure 7 shows each normalized ideal waveform of back EMF. Each back EMF waveform is applied to current waveform in Fig. 6 to calculate the torque ripple.

In Table 5, changes in the torque ripple according to the waveform of back EMF is shown. The result indicates that trapezoidal back EMF waveform lowers the torque ripple by 10% as compared to sinusoidal waveform at lower speed. In addition, speed ripple can also be lowered by trapezoidal back EMF waveform. Hence, the speed ripple of wheelchair can be reduced when back EMF waveform of traction motor is trapezoidal when simultaneously considering the current waveform.

Table 4 Circuit parameter information

	Value	Unit
Phase resistance	9.8	mΩ
Phase inductance	0.021	mH

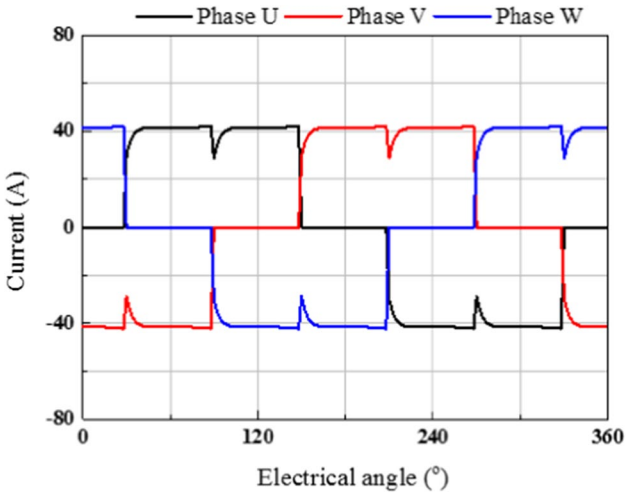

Fig. 6 Current waveform of BLDC motor at 200 rpm

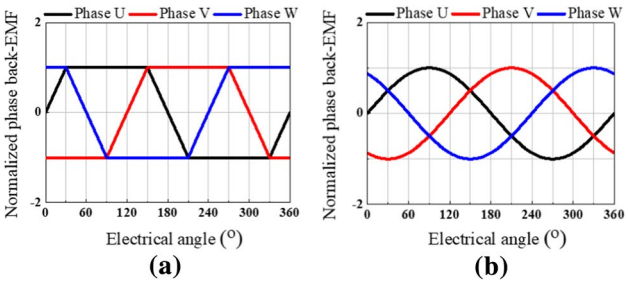

Fig. 7 Normalized waveform of back EMF **a** trapezoidal **b** sinusoidal

Table 5 Torque ripple and speed ripple by different type of back EMF waveform

Type of back EMF waveform	Torque ripple	Speed ripple	Unit
Trapezoidal	31.4	12.4	%
Sinusoidal	41.4	15.7	%

The summary of reducing torque ripple for ride comfort improvement by selecting electrical input is shown in Fig. 8. The speed ripple of electric wheelchair is affected by torque ripple at lower speed and the type of current waveform is nearly square wave. Therefore, selecting back EMF waveform as a trapezoidal form can lower the torque ripple of the traction motor. The motor design for trapezoidal back EMF waveform is discussed in the next section.

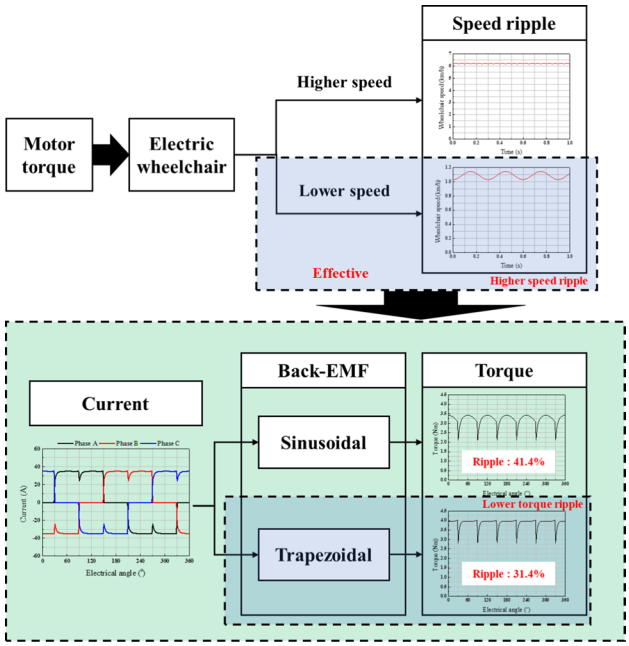

Fig. 8 Summary of reducing torque ripple by modifying electrical input

4 Design of BLDC Traction Motor

The design process of the traction motor for electric wheelchair is discussed in this section. To improve the ride comfort of the wheelchair, minimizing the torque ripple of the motor is the main objective of this process. The sensitivity of motor design parameters to motor performance is identified and the design variables for optimization are selected. Subsequently, the optimized model for traction motor is determined using kriging surrogate model.

4.1 Sensitivity Analysis

Among the design variables that are likely to affect the motor performance such as average torque and torque ripple of the traction motor, the variables that significantly affect those performances are selected by sensitivity analysis. The candidates for sensitivity analysis are shown in Table 6. PM is permanent magnet.

To identify the effect of design variables on the motor performance, the design of experiment should be constructed. This table was constructed using mixed orthogonal array [10, 11]. The number of experiments are 72. Each value in the table indicates the level of design experiment. Considering the nonlinearity of motor performance depending on the level of the design variable, the number of design variable level is determined as 3; from 0 to 2 [12]. However, the level of skew angle and the number of notches were determined as 2; from 0 to 1. The number of

Table 6 Design variables for sensitivity analysis

	Design variable		Design variable
x_1	Eccentricity	x_6	Notch depth
x_2	Notch width	x_7	PM thickness
x_3	Pole angle	x_8	Tooth tip
x_4	Slot opening	x_9	Skew angle
x_5	Tooth thickness	x_{10}	Number of notches

notches cannot exceed two notches because of the limited width of the stator teeth. The mechanical skew angle θ_s can be determined as (6) considering the period of cogging torque [13, 14]. LCM is the least common multiple, Q is number of slots, p is pole pair number, and s is the number of skew steps which is 2 in this design process. Because the skew angle for each DOE point is determined, the level of skew angle for DOE should be 2.

$$\theta_s = \frac{360}{s \cdot \mathrm{LCM}(2p, Q)} \tag{6}$$

The values of candidate design variables according to their each level are listed in Table 7. The design variables are represented in Fig. 9. The skew angle θ_s varies depending on the number of notches. Applying the information, the average torque and torque ripple of each DOE point is calculated using finite element analysis (FEA).

To select the design variable that significantly affect the average torque and torque ripple, analysis of variance (ANOVA) is applied using the calculated results. The p-values of each design variables are obtained through ANOVA. The design variable is considered as significant variable when p value is lower than significant level which value is 0.05 in this study [11]. Figure 10 shows the results of p value of design variable for average torque and torque ripple.

Table 7 Comparison of experimental and analytical results

Design variable	Level			Unit
	0	1	2	
Eccentricity	0	5	10	mm
Notch width	0.9	1.2	1.5	mm
Pole angle	39	41	43	°
Slot opening	0.9	1.2	1.5	mm
Tooth thickness	3.9	4.1	4.3	mm
Notch depth	0.2	0.4	0.6	mm
PM thickness	2.7	3.0	3.3	mm
Tooth tip	0.8	0.9	1.0	mm
Skew angle	0	θ_s		°
Number of notches	1	2		–

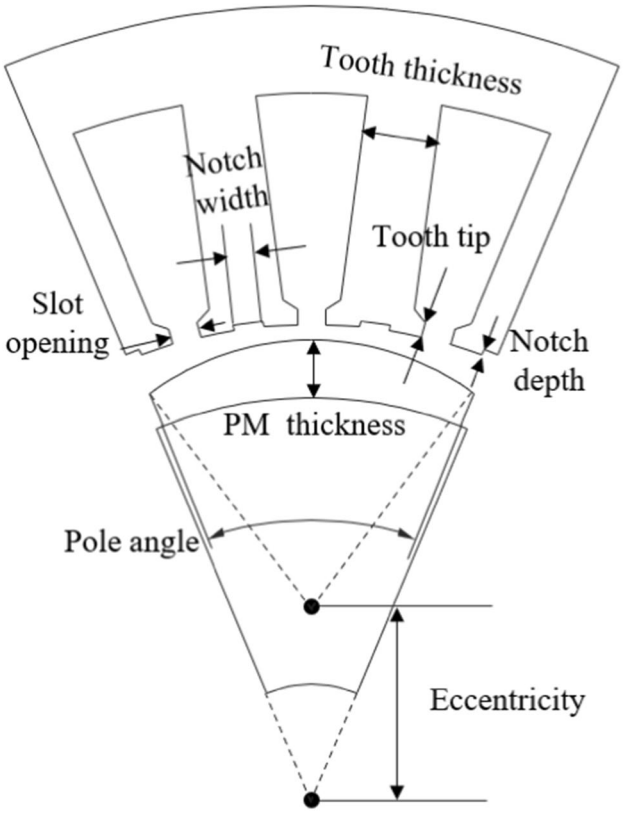

Fig. 9 Candidate design variables for sensitivity analysis

In case of average torque, the eccentricity (x_1) and thickness of PM (x_7) are below the significant level. The p values of notch width (x_2) and skew angle (x_8) were below the given significant level in case of the torque ripple. Thus, these 4 design variables are selected for traction motor optimization among 10 candidates.

4.2 Optimization

To minimize the torque ripple of the traction motor while maintaining certain amplitude average torque, the motor design variables selected in the former section should be optimized. The formulations for optimization are as follows. $\mathbf{x}$ is the vector of the normalized design variables, F is the objective function minimizing the torque ripple μ_R. G is the constraint indicating that the average torque of the motor μ_T should be at least 3 Nm.

$$\begin{aligned} &\text{Minimize } F(\mathbf{x}) = \mu_R(\mathbf{x}) \\ &\text{subject to } G(\mathbf{x}) = \mu_T(\mathbf{x}) \geq 3 \end{aligned} \tag{7}$$

This formulation needs to be applied to interpolated model to find the optimum point. In this study kriging surrogate model is used for optimization which is highly accurate for nonlinear functions [15]. To formulate the kriging

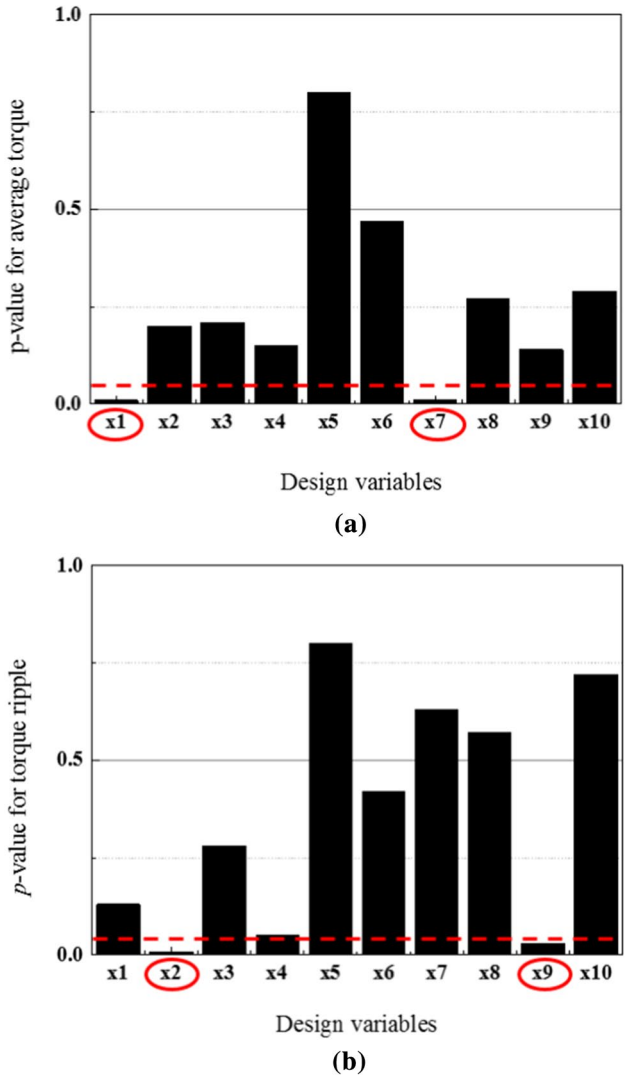

Fig. 10 *p*-values of design variables for **a** average torque and **b** torque ripple

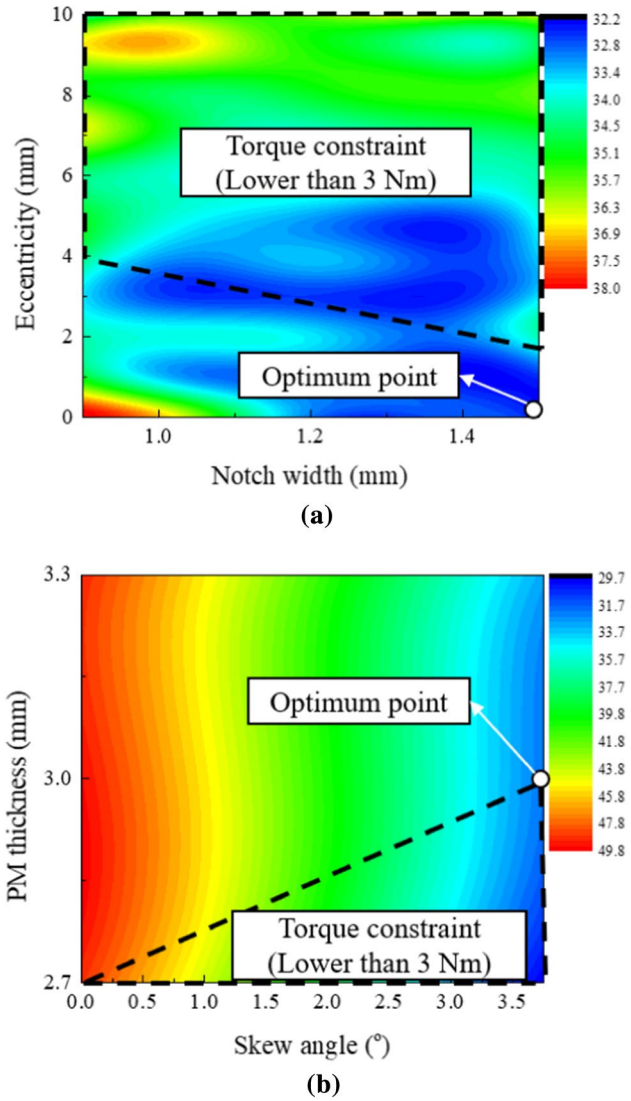

Fig. 11 Optimum point of design variables **a** notch width and eccentricity **b** skew angle and PM thickness

surrogate model, sampling points in the range of design variables are needed. The sampling points were generated by using Latin hypercube design (LHD) [16]. Sequential maximum distance design (SMDD) was also adopted for sampling [17]. As a result, 270 sampling points were generated by LHD and the average torque and torque ripple of each sampling point were calculated by FEA. The kriging surrogate model can be constructed by calculated results [18].

The validity of kriging model is evaluated leave-one-out cross-validation method [19]. The average torque and torque ripple predicted by this model is compared with calculated value using FEA. The normalized root mean square error (NRMSE) for verifying the accuracy of kriging surrogate model is as follows. $\mathbf{x}$ is the vector of design variables, $\mathbf{Y}(\mathbf{x})$ is the vector of motor performance, n_s is the number of sample points, $Y(x_i)$ is the motor performance at ith sample point predicted by surrogate model, and $Y(x_i)$ is the motor performance at ith sample point computed by FEA.

$$\mathrm{NRMSE} = \sqrt{\frac{1}{n_s} \cdot \sum_{i=1}^{n_s} \left(\frac{\hat{Y}^{-i}(x_i) - Y(x_i)}{\max(\mathbf{Y}(\mathbf{x}))} \right)^2} \cdot 100\% \qquad (8)$$

The NRMSE between calculated and predictive motor performance were 3% in case of average torque and 3.75% in case of torque ripple.

Then, considering the formulation of optimization in (7), the optimized motor model can be obtained from kriging surrogate model. The optimum point is shown in Fig. 11. The optimum point minimizing the torque ripple is

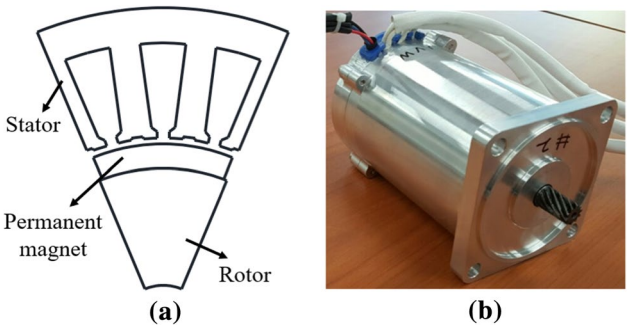

Fig. 12 Traction motor for electric wheelchair. **a** 2-D model, **b** manufactured motor

Table 8 Specifications of improved BLDC Motor

Categories	Value	Unit
Stack length	80	mm
Number of poles/slots	8/24	–
Number of turns per phase	11	–
Number of parallel circuits	4	–
Stator diameter	82	mm
Rotor diameter	47.5	mm
Residual induction of PM	1.22	T

determined. Considering the torque constraint, the eccentricity is 0 mm, and notch width should be 1.5 mm. The mechanical skew angle should be 3.75° and PM thickness should be at least 3 mm. Then the optimized traction motor for electric wheelchair is shown in Fig. 12 and its characteristics are listed in Table 8.

5 Experiment Result

This section covers the experiment results of back EMF waveform and torque ripple of designed motor. Figure 13 shows the experiment settings of BLDC traction motor for electric wheelchair. The back EMF and current waveform were measured using oscilloscope and probes, the rotating speed was measured by tachometer, and the torque was measured by torque transducer linked with hysteresis brake.

Rotating the designed motor at 200 rpm, the line-to-line back EMF waveform, the current waveform, and the torque ripple of the motor is shown in Figs. 14, 15, and 16 respectively. The back EMF waveform of the designed motor is trapezoidal as intended in design process. The experimental rms value is 6.01 V and calculated value is 5.94 V. The current waveform in Fig. 15 is similar to the current waveform calculated by simulation. The measured rms value is 32.4 A while the simulation result is 33.7 A.

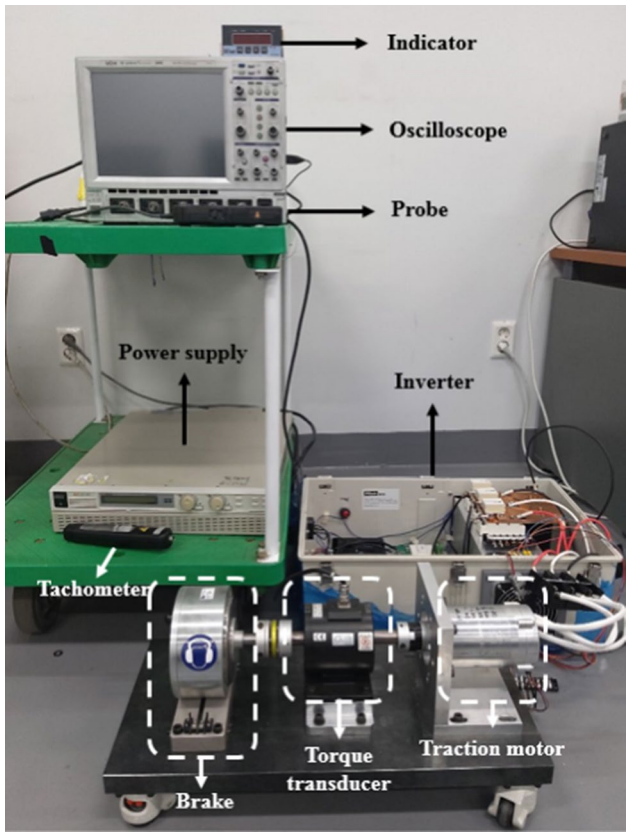

Fig. 13 Experiment settings of BLDC traction motor

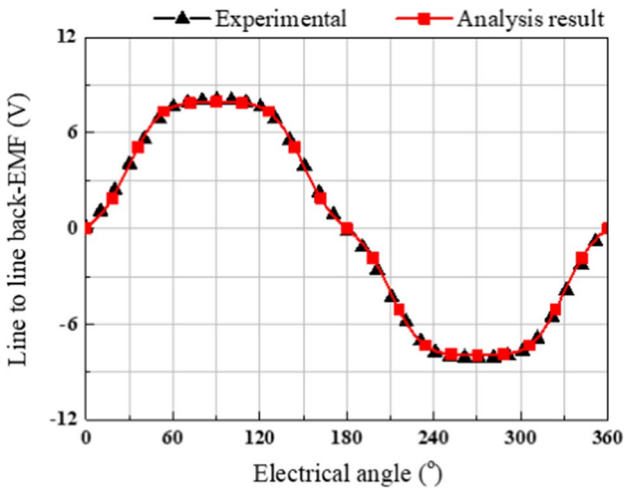

Fig. 14 Line to line back EMF waveform of designed BLDC motor

The average torque of experimental and analytical results are 2.99 Nm and 3.05 Nm respectively. The measured torque ripple is 23.3% and that of calculated by FEA is 32.4%. The overall results are in Table 9.

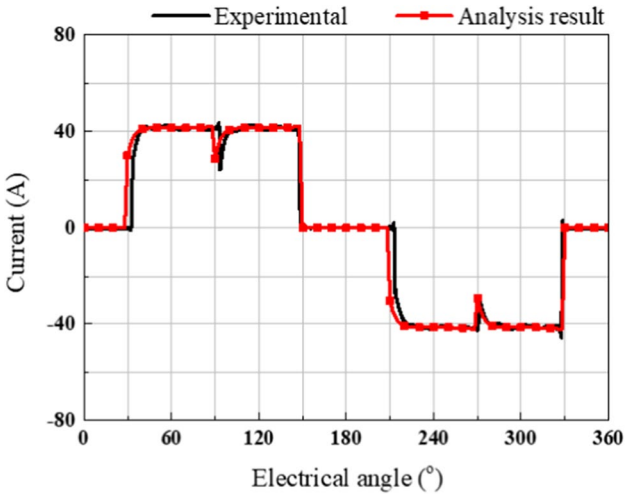

Fig. 15 Current waveform of designed BLDC motor

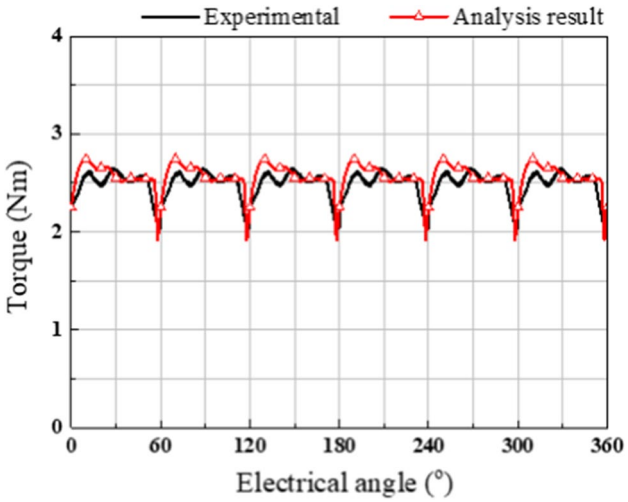

Fig. 16 Torque ripple of designed BLDC motor

Table 9 Specifications of improved BLDC Motor

Categories	Experimental results	Analytical results	Unit
Line to line back-emf (rms value)	6.01	5.94	V
Current (rms value)	32.4	33.7	A
Average torque	2.99	3.05	Nm
Torque ripple	23.3	32.4	%
Phase resistance	17.2	17.0	mΩ

6 Conclusion

This study discussed the method to improve the ride comfort by reducing the torque ripple. The relationship between the speed ripple and torque ripple was discussed by electric wheelchair modeling, and it clarified that reduction of torque ripple can reduce the fluctuation of wheelchair speed especially at lower speed. The current and back EMF waveform was also considered. The current waveform at 200 rpm of motor speed turned out to be nearly square wave and back EMF waveform was trapezoidal, because the speed ripple generated by that form is approximately 3% lower than that of sinusoidal form. Comparing the harmonic component of cogging torque with torque ripple of motor, reduction of cogging torque is effective in decreasing the torque ripple. The cogging torque is suppressed by notch and skew. Considering several cases with different number of notches and skew angle, the motor with single notch and 7.5° of skew angle reduced the speed ripple by 8.0% resulting in improvement in the ride comfort of electric wheelchair. This is verified through experiment.

Acknowledgements This work was supported by the National Research Foundation of Korea (NRF) grant funded by the Korea government (MSIT) (NRF-2020R1A4A4079701).

References

1. Seki H, Ishihara K, Tadakuma S (2009) Novel regenerative braking control of electric power-assisted wheelchair for safety downhill road driving. IEEE Trans Ind Electron 56(5):1393–1400
2. Seki H, Tanohata N (2012) Fuzzy control for electric power-assisted wheelchair driving on disturbance roads. IEEE Trans Syst Man Cybern C Appl Rev 42(6):1624–1632
3. Wu BF, Chen YS, Huang CW, Chang PJ (2018) An uphill safety controller with deep learning-based ramp detection for intelligent wheelchairs. IEEE Access 6:28356–28371
4. Jang G, Kim J, Lee S, Choi Y (2016) EMG-based continuous control scheme with simple classifier for electric-powered wheelchair. IEEE Trans Ind Electron 63(6):3695–3705
5. Shibata T, Murakami T (2012) Power-assist control of pushing task by repulsive compliance control in electric wheelchair. IEEE Trans Ind Electron 59(1):511–520
6. Yang YP, Huang WC, Lai CW (2017) Optimal design of rim motor for electric powered wheelchair. IET Electr Power App 1(5):825–832
7. *Rules for users of powered wheelchairs and mobility scooters (36 to 46)*," Aug. 20, 2019. Accessed on : Sept. 11, 2019. [Online]. Available: https://www.gov.uk/guidance/the-highway-code/rules-for-users-of-powered-wheelchairs-and-mobility-scooters-36-to-46
8. *Products-robo3.com* (2019) Accessed on: Sept. 11, 2019. [Online]. Available: https://www.robo3.com/products/
9. Chen CH, Cheng MY (2007) A new cost effective sensorless commutation method for brushless DC motors without phase shift circuit and neutral voltage. IEEE Trans Power Electron 22(2):644–653

10. "*Orthogonal Arrays*," Jan. 29, 2019. Accessed on: Oct. 24, 2020. [Online]. Available: http://neilsloane.com/oadir/
11. Montgomery DC (2017) Simple comparative experiments. In: Design and analysis of experiments, vol 2, 9th ed., John Wiley & Sons, New York, pp 35
12. Cho GW, Jang WS, Jang KB, Kim GT (2012) The optimal design of fractional-slot SPM to reduce cogging torque and vibration. JEET 7(5):753–758
13. Azar Z, Zhu ZH, Ombach G (2012) Investigation of torque-speed characteristics and cogging torque of fractional-slot IPM brushless AC machines having alternate slot openings. IEEE Trans Ind Appl 48(3):903–912
14. Fei W, Zhu ZQ (2013) Comparison of cogging torque reduction in permanent magnet brushless machines by conventional and herringbone skewing techniques. IEEE Trans Energy Convers 28(3):664–674
15. Lebensztajn L, Marretto CAR, Costa MC, Coulomb JL (2004) Kriging: a useful tool for electromagnetic device optimization. IEEE Trans Magn 40(2):1196–1199
16. Sacks J, Welch WJ, Mitchell TJ, Wynn HP (1989) Design and analysis of computer experiments. J Stat Sci 40(4):409–423
17. Kim S, Lee SG, Kim JM, Lee TH, Lim MS (2020) Uncertainty identification method using kriging surrogate model and Akaike information criterion for industrial electromagnetic device. IET Sci Meas Technol 14(3):250–258
18. Lee TH, Jung JJ (2007) "Kriging meta model based optimization", in Optimization of structural and mechanical systems, vol 16. World Scientific Publishing Co., Singapore, pp 445–484
19. Queipo NV, Haftka RT, Shyy W, Goel T, Vaidyanathan R, Tucker PK (2005) Surrogate-based analysis and optimization. Prog Aerospace Sci 41(1):1–8

Publisher's Note Springer Nature remains neutral with regard to jurisdictional claims in published maps and institutional affiliations.

Dae-Kee Kim received Bachelor's degree in mechanical engineering from Hanyang University, Seoul, South Korea, in 2014. Currently he is pursuing a Ph.D. degree in automotive engineering in Hanyang University, Seoul, South Korea. His research interests are the design and optimization of electric machines and analysis of vibration generated by electric machines.

Dong-Min Kim received the B.S. degree in electronic system engineering, and the Ph.D. degree in automotive engineering from Hanyang University, Seoul, South Korea, in 2013 and 2021, respectively. In 2021, he was a Postdoctoral Researcher in Hanyang University, Seoul, South Korea. Since 2021, he has been with Honam University, Gwangju, South Korea, where he is currently an Assistant Professor. His research interests include design optimization of electric machines for automotive and industrial applications, modeling and optimization of electric vehicles, hybrid electric vehicles, and fuel cell electric vehicles.

Jin-Cheol Park received a Bachelor's degree in electrical engineering from Chungbuk University, Cheongju, Korea, in 2015 and a Master's degree in automotive engineering from Hanyang University, Seoul, Korea, in 2017. Currently he is pursuing a Ph.D. degree in automotive engineering from Hanyang University, Korea. His main research is electric machine design for automotive electric machine drive for industrial applications.

Soo-Gyung Lee received the bachelor's degree in electrical engineering from Konkuk University, Seoul, South Korea, in 2014. And, she recieved the Ph.D degree in automotive engineering from Hanyang University, Seoul, South Korea, in 2021. Currently, she is a Senior Researcher with POSCO, Incheon, South Korea. Her research interests include the design and optimization of electical machines.

Jihyung Yoo received his Bachelor's degree in mechanical engineering from Hanyang University, Seoul, South Korea in 2005. He received his Master's and Ph.D. degree at Stanford university in 2007 and 2011, respectively. From 2011 to 2013 he was a postdoctoral researcher at the National Transportation Research Center at Oak Ridge National lab. From 2013 to 2017 he was an assistant professor in the department of Mechanical and Aerospace Engineering at The State University of New York at Buffalo. Since 2017, he has been with Hanyang University, where he is currently an associate professor. His research interests include optical sensing and thermofluidic analysis of automotive and aeronautical energy systems such as electric motors, battery packs, and turbines.

Myung-Seop Lim received the Bachelor's degree in mechanical engineering from Hanyang University, Seoul, South Korea, in 2012. Also, he received the Master's and Ph.D. degree in automotive engineering from the same university, in 2014 and 2017, respectively. From 2017 to 2018, he was a Research Engineer in Hyundai Mobis, Yongin, South Korea. From 2018 to 2019, he was an Assistance Professor in Yeungnam University, Daegu, South Korea. Since 2019, he has been with Hanyang University, Seoul, South Korea, where he is currently an Assistant Professor. His research interests include electromagnetic field analysis and multi-physics analysis of electric machinery for mechatronics systems such as automotive and robot applications.